International Journal of Engineering, Mathematical and Physical Sciences
ISSN: 2517-9934
Vol:7, No:12, 2013

Intelligent Face-Up CMP System Integrated with On-Line Optical Measurements

Sheng-Ming Huang, Nan-Chyuan Tsai, Chih-Che Lin, Chun-Chi Lin

***Abstract*—**An innovative design for intelligent Chemical Mechanical Polishing (CMP) system is proposed and verified by experiments in this report. On-line measurement and real-time feedback are integrated to eliminate the shortcomings of traditional approaches, e.g., the batch-to-batch discrepancy of required polishing time, over consumption of chemical slurry, and non-uniformity across the wafer. The major advantage of the proposed method is that the finish of local surface roughness can be consistent, no matter where the inner-ring region or outer-ring region is concerned. Secondly, it is able to eliminate the Edge effect. Conventionally, the interfacial induced stress near the wafer edge is generally much higher than that near the wafer center. At last, by using the proposed intelligent chemical mechanical polishing strategy, the cost of the entire machining cycle can be much reduced while the quality of the finished goods certainly upgraded.

***Keywords*—**Chemical Mechanical Polishing, Active Magnetic Actuator, On-Line Measurement.

I. Introduction

CHEMICAL MECHANICAL POLISHING (CMP) is a widely used technique in the manufacture of advanced multilayer integrated circuits (ICs) for achieving global planarity of wafer surfaces. In commonly employed CMP process, the material removal task is accomplished by pressing a face-down wafer into a relatively soft polymeric pad flooded with slurry. In addition, the polishing pad and wafer are both rotated in similar but different angular speeds so that every spot on the wafer can be polished at relative velocity to achieve uniform surface roughness. However, in fact, the main shortcomings of current CMP system in semiconductor industries are: non-uniform surface roughness and batch-to-batch discrepancy of required polishing time. As to the non-uniform surface roughness, it mainly stems from *Edge Effect*. One of the main factors for edge effect is *Von Mises* stress, which is a kind of composite axial stress. Therefore, in general the interfacial induced stress near the wafer edge is much higher than that near the wafer center [1]. On the other hand, by conventional approach the batch-to-batch discrepancy of required polishing time always exits and is determined by a few operational parameters, e.g., wear of pad and amount of abrasive particles so that the polishing time cannot be consistent. Therefore, an on-line terminal-point measurement methodology is proposed in this work. Though several methods of on-line terminal-point measurement, e.g., motor current (MC) method [2], [3], pad temperature detection [4], [5] and optical detection [6], [7] were reported, a certain degree of drawback exists such as the signal-to-noise ratio for the measured current or the variable temperature being too low to ensure sufficient measurement accuracy. On the other hand, if optical detection method is applied, the non-uniformity of surface roughness still cannot be compensated simultaneously.

Sheng-Ming Huang, Chih-Che Lin, and Chun-Chi Lin are with the Department of Mechanical Engineering, National Cheng Kung University, Tainan 70101, Taiwan (e-mail: n16004802@mail.ncku.edu.tw, n1897137@mail.ncku.edu.tw, n18991380@mail.ncku.edu.tw, respectively).

Nan-Chyuan Tsai is with the Department of Mechanical Engineering, National Cheng Kung University, Tainan 70101, Taiwan (corresponding author to provide phone: +886-6-2757575 Ext. 62137; fax: +886-6-2369567; e-mail: nortren@mail.ncku.edu.tw).

Based on the above-mentioned shortcomings, an innovative intelligent chemical mechanical polishing system is proposed in this work. The proposed system mainly consists of three laser displacement sensors and an active electromagnetic-type normal press module. By using tri-point measurement method onto the face-up wafer, the surface roughness of wafer can be on-line measured to quantify the degree of the non-uniformity of specific regions. In addition, the non-uniformity can be on-line compensated by the active electromagnetic-type normal press module.

II. Intelligent Chemical Mechanical Polishing System

A. Design of Innovative CMP System

An innovative Chemical Mechanical Polishing (CMP) system, shown in Fig. 1, is proposed in this paper. The structure of proposed CMP system is composed by a set of active electromagnetic-type (EM-type) normal press module, an actively movable pillar, three laser displacement sensors, a pair of preset constant pressure units, a lapping platen, a wafer carrier, a flexible coupler, a linear motor and an inductive motor. Before the polishing process is engaged, the lapping platen is moved to the top, shown in Fig. 2 (a), so that the face-up wafer can be conveniently placed on the wafer carrier and then fixed up. On the other hand, the polishing pad is set up at the bottom of lapping platen. During the polishing process, the lapping platen is moved downward, shown in Fig. 2 (b), to generate a constant pressure between the wafer and polishing pad. The wafer carrier is rotated by the inductive motor but the lapping platen is fixed and not rotated an all. In other words, the polishing pad is stationary in this work. On the right-hand side of lapping platen, the rectangular slot, shown in Fig. 3, is constructed so that the light emitted by three laser displacement sensors can penetrate onto the face-up wafer surface to measure the surface roughness of wafer. On the left-hand side of lapping platen, the movable pillar moves along the rectangular groove by a linear motor. By the EM-type normal press module, the movable pillar can be pushed downward to enhance the exerted pressure such that the specific non-uniform region of the wafer

can be compensated to improve its flatness. Furthermore, in order to overcome the incomplete fill-up of slurry between the wafer and polishing pad, the slurry is directly injected into the center of wafer through the passage of lapping platen.

B. Roughness of Wafer Surface by Tri-Point Measurement

In this work, the method of tri-point measurement, which consists of three laser displacement sensors, is employed. The structure and operation principle of laser displacement sensor for Keyence LK-H155 is shown in Fig. 4. The laser light reflected by a plane passes through the receiving lens on the position sensitive detector (PSD).

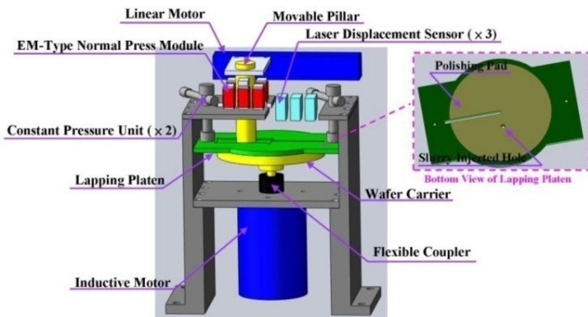

Fig. 1 Innovative design of CMP system

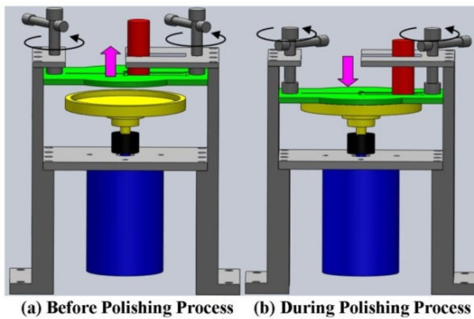

Fig. 2 Operational diagram of constant pressure units

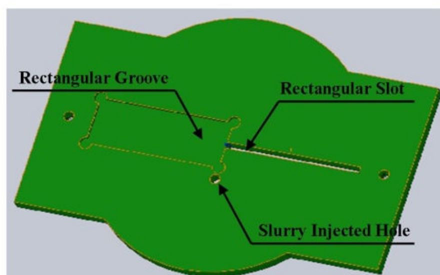

Fig. 3 Schematic diagram of lapping platen

By PSD-type sensors, the center of reflected light beam spot determines to generate the corresponding voltage with respect to the actual plane. Base on triangulation principle, the relation between the distance variation of the light beam spot on the PSD, Δd , and the displacement variation between the actual plane and expected plane, Δz , can be expressed as follows:

$$\Delta d / \Delta z = f \sin\theta / \rho \cos\alpha \qquad (1)$$

where f is the distance between PSD and light receiving lens, ρ the distance between the light receiving lens and "O" (i.e., the intersection point of reflected light by the expected plane and the emitting light by the semiconductor laser), θ the reflected angle for the actual plane with respect to the emitting light, and α the angle between the reflected lights of expected plane and actual plane. Finally, the distance variation of the beam spot on the PSD is transduced to a voltage signal by the associated circuit and amplifier board. The induced voltage signal, ΔV , can be represented as follows:

$$\Delta V = A \times \Delta d = A \times \Delta z (f \sin\theta / \rho \cos\alpha) \qquad (2)$$

where A is the overall gain of the circuit and amplifier board.

Basically, three laser displacement sensors are employed to constitute a set of tri-point measurement so that the roughness of wafer surface can be on-line measured. By three high-precision step motors, three laser displacement sensors are separately rotated to repeatedly scan the wafer along the radial direction. At first, the distance between the semiconductor laser and expected surface, z , is defined and shown in Figs. 4 and 5 (a). Furthermore, the distances between each laser displacement sensor and expected surface, i.e., $D_i(\beta_i)$, $i = a, b, c$ is also defined with respect to the variable rotated angle. According to triangulation principle, based on the rotated angle of each laser sensor, β_i , and its actual distance, $D_i'(\beta_i)$, the surface roughness of wafer can be measured, by scanning operation of these three laser displacement sensors. If all actual distances, $D_i'(\beta_i)$, $i = a, b, c$ are equal to their corresponding expected distances, $D_i(\beta_i)$, with respect to a specific spot, the roughness of this spot is achieved.

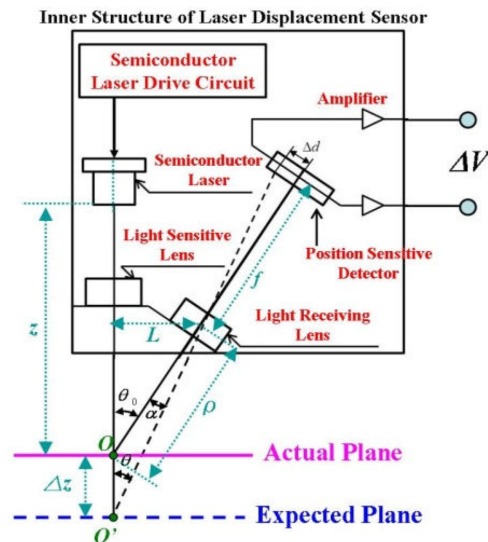

Fig. 4 Operational principle of laser displacement sensor

On the contrary, taking Fig. 5 (b) as an illustrative example, even if $D_a'(\beta_a)$ and $D_a(\beta_a)$ by *Sensor #a* are identical, but $D_b'(\beta_b)$ and $D_c'(\beta_c)$ are less than their corresponding ideal distances, $D_b(\beta_b)$ and $D_c(\beta_c)$, respectively. Therefore, it can be judged that the RHS neighborhood of Point "P" is still required to further polish its surface roughness by an active electromagnetic-type normal press module until $D_b'(\beta_b) = D_b(\beta_b)$ and $D_c'(\beta_c) = D_c(\beta_c)$ both hold. Similarly, Point "Q", shown in Fig. 5 (c), can also be polished to achieve the expected roughness based on feedback of the tri-point measurements: $D_a'(\beta_a)$, $D_b'(\beta_b)$ and $D_c'(\beta_c)$. The so called surface roughness, R_a, in this report can be evaluated by the method of central average surface roughness [8]. That is,

$$R_a = (|Y_1| + |Y_2| + \cdots + |Y_n|)/n \qquad (3)$$

where n is the number of samples and Y_n the surface roughness of the n-th sample.

III. Electromagnetic-Type Normal Press Module

A novel electromagnetic-type normal press module, which is basically an active magnetic actuator, is applied in our work. The major advantages of applying the proposed EM-type normal press module includes: (a) to compensate the local surface roughness of wafer, (b) to overcome the *Edge effect*, and (c) to reduce the required polishing time. The efficacy of the EM-type normal press module is verified by later-on intensive computer simulations and realistic experiments.

A. Material Removal Rate (MRR)

The Material Removal Rate (MRR) is determined by many parameters, e.g., the press force applied onto the wafer, the angular velocities of wafer and polishing pad, hardness of pad, abrasive particles of slurry and etc. Based on these parameters, the most common MRR equation, so-called Preston's equation [9], has been often employed and can be expressed as follows:

$$MRR = K_p \cdot (F / A_p) \cdot v \text{ for "hard" polishing pad} \qquad (4)$$

where K_p is Preston's coefficient, F the polishing force, A_p the polishing surface, and v the relative velocity between the wafer surface and the pad. On the other hand, the MRR equation for *"soft"* polishing pad was reported by Zhao and Shi [10]:

$$MRR = K_p \cdot (P^{2/3} - P_{th}^{\ 2/3}) \cdot v \text{ for "soft" polishing pad} \qquad (5)$$

where P is the polishing pressure and P_{th} the threshold pressure. It is noted that the polishing pressure has to be greater than the threshold pressure so that the material of wafer surface can be removed. However, in realistic world, either the polishing pressure or the threshold pressure is variant and real-time affected by the actual contact polishing surface between soft pad/wafer and the sandwiched abrasive particles.

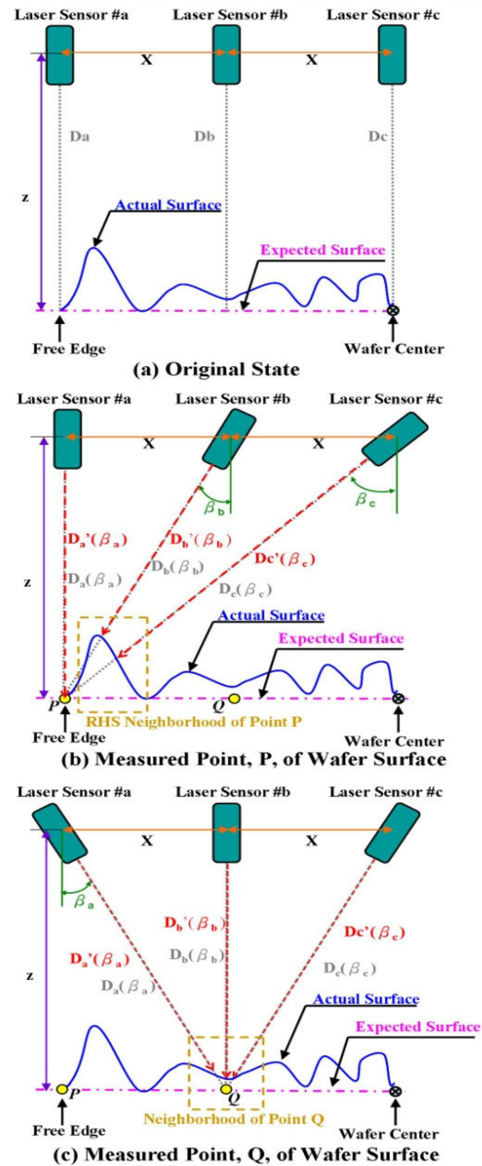

Fig. 5 Operational principle of tri-point measurement

Therefore, in this work, the MRR equation is modified as follows:

$$MRR = K \cdot (\varphi_1 P^{2/3} - \varphi_2 P_{th}^{\ 2/3}) \cdot v \qquad (6)$$

where φ_1 and φ_2 are modified factors obtained by the experimental tests.

B. Electromagnetic-Type Normal Press Module

In order to eliminate *edge effect* during the polishing process, an innovative electromagnetic-type normal press module, shown in Fig. 6 (a), is proposed in this paper. The EM-type normal press module consists of six I-shape electromagnets and

a movable pillar in which silicon steel is embedded to construct the closed-loop magnetic circuit. These six EM poles are organized into three sets (i.e., A1-A2, B1-B2 and C1-C2, shown in Fig. 6 (a)). As the electric current is applied to a set of wound coils at the press module, the magnetic force can be induced to move the movable pillar in vertical direction, shown in Fig. 6 (b). On the other hand, the horizontal position of movable pillar is controlled by a linear motor. Based on the horizontal position of movable pillar and its polar angle with respect to wafer, the entire wafer surface can be divided into 72 zones and shown in Fig. 7. By the EM-type normal press module, the polishing pressure for one of 72 zones can be enhanced to improve the non-uniform surface roughness.

By employing the commercial software, Maxwell Ansoft, the induced magnetic attractive forces in vertical direction are evaluated under various drive currents applied to the EM-type normal press module. From Fig. 8, it is found that the maximum flux density is about $1.968 Tesla$ as the applied current is $2.5A$ and the number of coil windings $400 turns$.

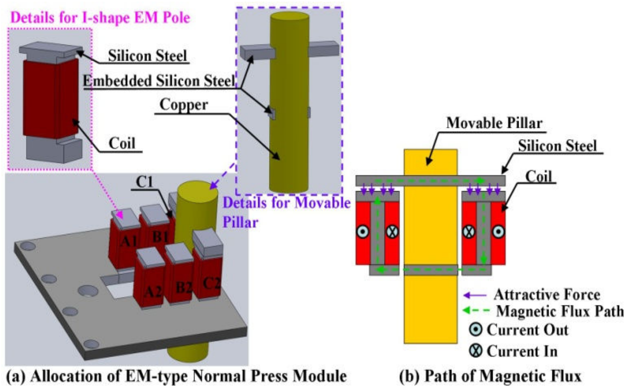

Fig. 6 Electromagnetic-type normal press module

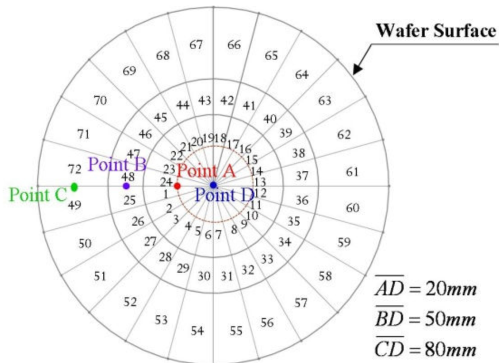

Fig. 7 72 Zones for wafer surface

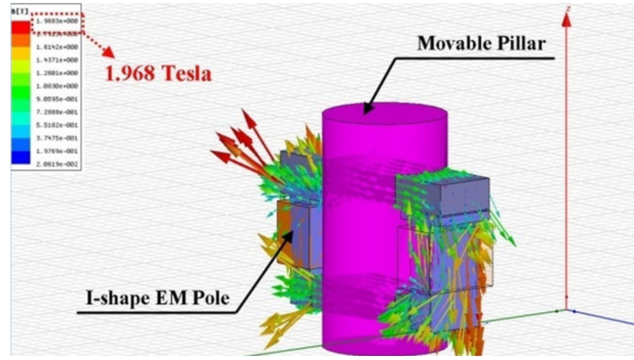

Fig. 8 Magnetic field distribution

On the other hand, the resulted induced attractive force under various drives current is shown in Fig. 9. From Fig. 9, the induced attractive force is approximately proportional to the square of applied current and it is also verified by later-on experiments. In addition, from the side-view of lapping platen, it can be approximated by a simply supported beam under a point load, shown in Fig. 10, such that Euler beam theory [11] can be applied to describe the deflection of lapping platen:

$$y = (bF/6EIL)(x^3 - S^2x + b^2x) - (F/6EI)(x-a)^3 \qquad (7)$$

where y is the deflection of lapping platen, x the distance between the movable pillar and the left free end, E the Young's modulus, I the principal second moment of inertia. The physical values of these parameters are summarized in Table I. The deflection of lapping platen versus the induced attractive force by the EM-type normal press module at three specific points (i.e., Point A, B and C in Fig. 7) can be obtained by FEM software, *Working Model*, and shown in Fig. 11. It is also compared with the numerical solution of (7): hereafter called GEA (Governing Equations Analysis). It is found that the results by GEA and FEM approaches are, to some extent, similar.

TABLE I
PHYSICAL VALUES OF SYSTEM PARAMETERS

Design Parameter	Physical Value
Diameter of Wafer Carrier, S	0.26m
Thickness of Lapping Platen, T	0.01m
Mass of Lapping Platen, m	3.77kg
Young's modulus, E	2×10^{12} Pa

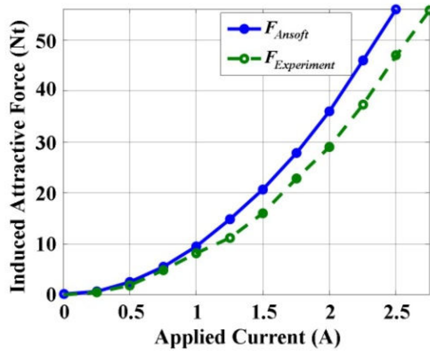

Fig. 9 Induced attractive force under various applied current

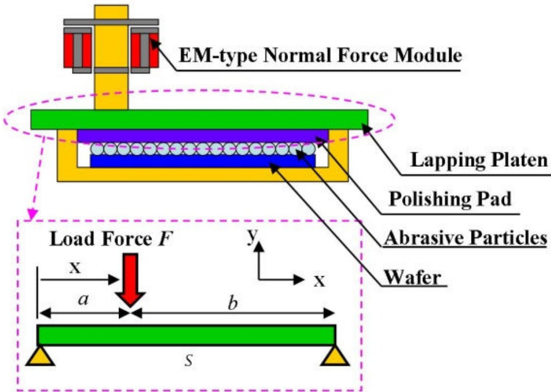

Fig. 10 Diagram of a simply supported beam under a point load

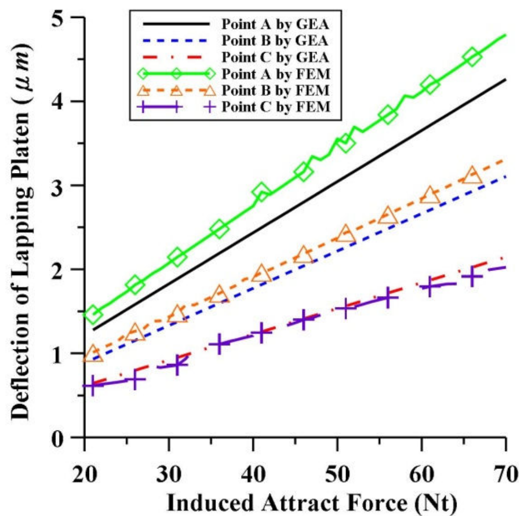

Fig. 11 Deflection of lapping platen under various induced attractive force

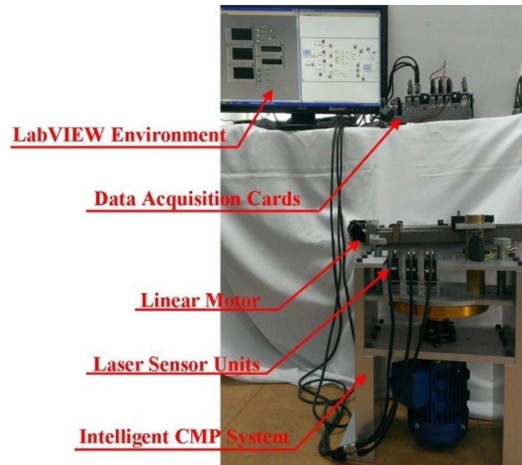

Fig. 12 Photo of intelligent CMP system

IV. Experimental Results and Analysis

The test rig of the intelligent chemical mechanical polishing system is shown in Fig. 12. The experiments are undertaken by using the NI 9215 data acquisition (DAQ) card under *LabVIEW* environment by *National Instruments*. The inductive motor is energized by applying 3-phase AC current to rotate the wafer carrier at $120\,RPM$. In order to suppress potentially severe eccentricity effect, the wafer carrier is beforehand calibrated by dynamic balancer at first, shown in Fig. 13. The roughness of wafer surface is on-line measured by three laser displacements sensor units. The schematic diagram for the proposed intelligent closed-loop system is shown in Fig. 14. In this work, a fuzzy PID controller is employed to control the EM-type normal press module based on the error between the expected roughness surface and the actual roughness surface. In order to clearly demonstrate the efficacy of the proposed intelligent CMP system, the wafer is replaced by an aluminum disc in the follow-up experiments. The check points are set at Points A, B and C, shown in Fig. 7. The roughness of aluminum disc before polishing process is shown in Fig. 15. The surface roughness of Points A, B and C, based on (3), are about $12.6\,\mu m$, $6.1\,\mu m$ and $11.2\,\mu m$ respectively.

Fig. 13 Wafer carrier and dynamic balancing

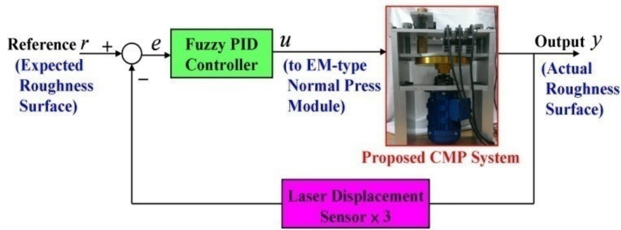

Fig. 14 Block diagram of proposed intelligent control system

After polishing process, the surface roughness of Points A, B and C are about $1.5\,\mu m$, $2.2\,\mu m$ and $2.4\,\mu m$ respectively and shown in Fig. 16. The OMEs (Optic Microscope Images) of the roughness of aluminum disc before/after polishing process are shown in Fig. 17. From Figs. 15 and 16, the surface roughness can be reduced by 88% under the proposed intelligent CMP strategy.

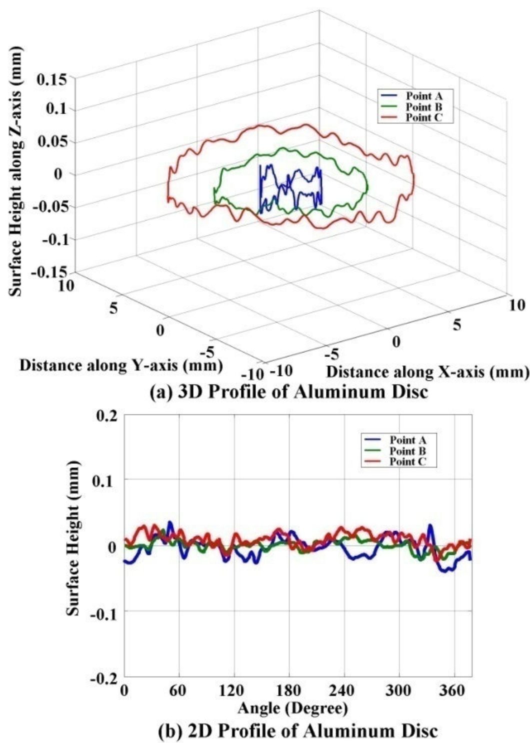

Fig. 15 Measured roughness of aluminum disc before polishing process engaged

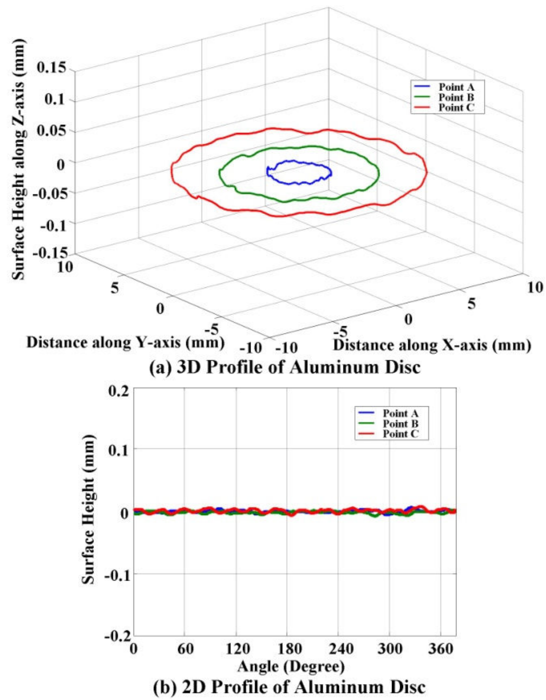

Fig. 16 Measured roughness of aluminum disc after polishing process completed

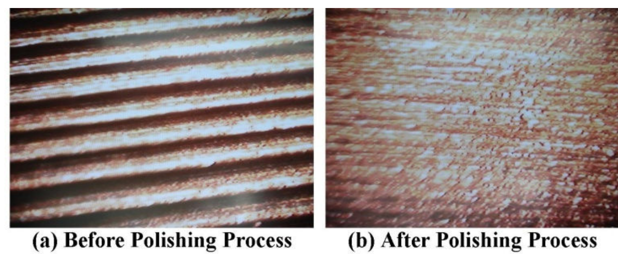

Fig. 17 OM images of roughness of aluminum disc before/after polishing process

V. CONCLUSION

An innovative intelligent chemical mechanical polishing system, which consists of three laser displacement sensors and a novel electromagnetic-type (EM-type) normal press module, is designed and presented in this paper. By the tri-point measurement method, the local surface roughness of wafer can be on-line evaluated. Based on the measurement, an induced magnetic force by the novel EM-type normal press module is exerted to the movable pillar in vertical direction so that the over-height roughness of specific regions can be particularly polished. By applying commercial softwares, *Ansoft Maxwell* and *Working Model*, the efficacy of the EM-type normal press module is verified. From the simulation results, the maximum flux density is about $1.968\,Tesla$ as the applied current is $2.5A$. In addition, the deflection of lapping platen versus the induced magnetic attractive force by finite element method and governing equations analysis is, to some extent, similar. Finally, an experimental test rig is set up to verify the efficacy

of the proposed intelligent chemical mechanical polishing system. From experiment results, the surface roughness can be reduced by 88% under the proposed fuzzy PID control strategy.

ACKNOWLEDGMENT

This research was partially supported by National Science Council (Taiwan) with Grant 102-ET -E-006 -007 -ET and the authors would like to express their appreciation.

REFERENCES

[1] D. Wang, J. Lee, K.T. Bibby, S. Beaudoin and T. Cale, "Von Mises Stress in Chemical-Mechanical Polishing Processes," *J. Electrochem. Soc.*, Vol. 144, pp. 1121-1127, 1997.

[2] J. Sorooshian, A. Philipossian, D. Stein, R. Timon and D.L. Hetherington, "Dependence of Oxide Pattern Density Variation on Motor Current Endpoint Detection during Shallow Trench Isolation Chemical Mechanical Planarization," *Japanese Journal of Applied Physics*, Vol. 44, pp. 1219-1224, 2005.

[3] C. Xu, D.M. Guo, Z.J. Jin and R.K. Kang, "A Signal Processing Method for the Friction-based Endpoint Detection System," *Journal of Semiconductors*, Vol. 31, pp. 126002, 2010.

[4] H.C. Hong and Y.L. Huang, "In Situ Endpoint Detection by Pad Temperature in Chemical-Mechanical Polishing of Copper Overlay," *IEEE Transactions on Semiconductor Manufacturing*, Vol. 17, pp. 180-187, 2004.

[5] L.J. Chen, Y.L. Huang, Z.H. Lin and H.W. Chiou, "Pad Thermal Image End-pointing for CMP Process," *CMP-MIC Conference*, pp. 28-35, 1998.

[6] D.A. Chan, B. Swedek, A. Wiswesser and M. Birang, "Process Control and Monitoring with Laser Interferometry Based Endpoint Detection in Chemical Mechancial Planarization," *IEEE/SEMI Advanced Semiconductor Manufacturing Conference*, pp. 377-384, 1998.

[7] H.C. Hong and Y.L. Huang, "A Comprehensive Review of Endpoint Detection in Chemical Mechanical Planarization for Deep-submicron Integrated Circuits Manufacturing," *Int. J. Nano Technology*, Vol. 3B2, pp. 1-18, 1999.

[8] E.P. DeGarmo, *Materials and Processes in Manufacturing*, 9th ed, New Jerse: Wiley, 2003.

[9] F.W. Preston, "The Theory and Design of Plate Glass Polishing Machines," *J. Soc. Glass Tech.*, Vol. 11, pp. 214-257, 1927.

[10] B. Zhao and F.G. Shi, "Chemical Mechanical Polishing: Threshold Pressure and Mechanism," *Electrochemical and Solid-State Letters*, Vol. 2, pp. 145-147, 1999.

[11] H.P. Lee, "Dynamic Response of a Beam with Intermediate Point Constraints Subject to a Moving Load," *Journal of Sound and Vibration*, Vol. 171, pp. 361-368, 1994.